

Journal of Materials Chemistry B

Accepted Manuscript



This is an *Accepted Manuscript*, which has been through the Royal Society of Chemistry peer review process and has been accepted for publication.

Accepted Manuscripts are published online shortly after acceptance, before technical editing, formatting and proof reading. Using this free service, authors can make their results available to the community, in citable form, before we publish the edited article. We will replace this *Accepted Manuscript* with the edited and formatted *Advance Article* as soon as it is available.

You can find more information about *Accepted Manuscripts* in the [Information for Authors](#).

Please note that technical editing may introduce minor changes to the text and/or graphics, which may alter content. The journal's standard [Terms & Conditions](#) and the [Ethical guidelines](#) still apply. In no event shall the Royal Society of Chemistry be held responsible for any errors or omissions in this *Accepted Manuscript* or any consequences arising from the use of any information it contains.

ARTICLE

Micelle-like Luminescent Nanoparticles as a Visible Gene Delivery System with Reduced Toxicity

Cite this: DOI: 10.1039/x0xx00000x

Keni Yang, †^{ab} Shengliang Li, †^a Shubin Jin, ^a Xiangdong Xue, ^a Tingbin Zhang, ^a Chunqiu Zhang, ^{*a} Jing Xu ^{*a} and Xing-Jie Liang ^{*a}

Received 00th January 2012,

Accepted 00th January 2012

DOI: 10.1039/x0xx00000x

www.rsc.org/

Cationic polymers have been widely used as promising non-viral gene carriers, but their undesirable toxicity is a drawback. Hydrophobic modification has been developed as an efficient strategy to overcome this disadvantage. In this study, 25 kDa polyethyleneimine (PEI), the gold standard of polycations for effective gene delivery, was modified with the hydrophobic luminogen tetraphenylethene (TPE), which shows aggregation-induced emission (AIE) and has been utilized as a luminescent probe in various applications. The modified PEI (TPEI) self-assembled into micelle-like nanoparticles (TPEI-NPs) and displayed AIE behavior in aqueous media. The TPEI-NPs exhibited bright blue fluorescence and were suitable for long-term cell imaging. Compared with PEI, TPEI-NPs showed lower cytotoxicity but the transfection efficiency was nearly high. Therefore, modification of polycations with hydrophobic fluorescent molecules represents an advanced strategy for designing visible gene vehicles with low toxicity.

Introduction

Gene therapy has become a promising strategy for treatment of diseases ranging from hereditary disorders to acquired illness.¹ The soaring interests and rapid progress in gene therapy benefit from the development of gene delivery systems.² Cationic polymers, one of the most important non-viral gene delivery systems, have attracted intense research efforts due to their facile manufacture, flexibility, stability and proven gene delivery efficiency.^{3,4} However, low transfection efficiency and undesirable cytotoxicity are still the greatest obstacles preventing the clinical application of polycations.⁵ A wide range of modifications have been implemented to tackle these disadvantages while maintaining or improving the gene delivery efficiency, among which hydrophobic conjugation exhibits great promise.⁶ As shown in previous research, the addition of hydrophobic segments can influence the formation and stability of complexes formed by carriers and nucleic acids,⁷ and the interaction between hydrophobic groups and the lipophilic cell membrane improves the compatibility of complexes as they cross the plasma membrane, thus enhancing cellular uptake.⁸ These properties all contribute to more efficient gene transfer with reduced cytotoxicity.

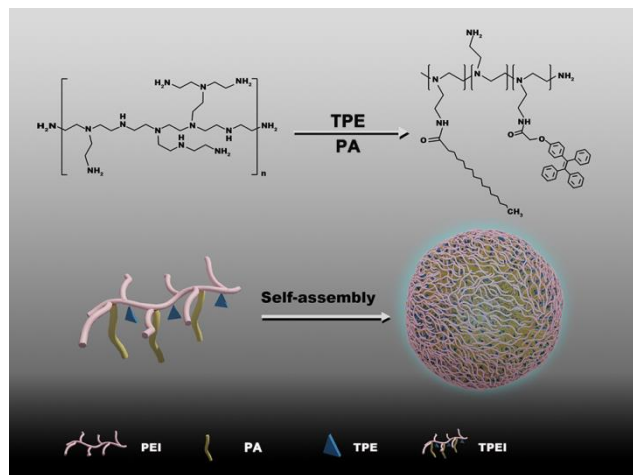
Traditional cationic gene delivery systems lack a suitable signal for long-term and real-time imaging of the process of gene transfer.⁹ In order to monitor gene delivery and release for the improvement of current gene therapy protocols, carriers can be modified with fluorescent reagents and tracked through fluorescence microscope.¹⁰ However, fluorescent dyes often suffer from the aggregation-caused quenching (ACQ) effect¹¹ and poor photostability,¹² which decrease their suitability for

this purpose. These limitations can be overcome by using quantum dots (QDs), which have been reported as a dual modal gene delivery carrier and imaging agent thanks to their unique optical properties. However, the intrinsic toxicity of QDs in oxidative biological environments hinders their further applications.^{13,14}

The unique phenomenon of aggregation-induced emission (AIE) holds great promise for the development of novel fluorescent agents.¹¹ An AIE fluorophore is almost non-emissive in a monodisperse state but emits efficiently when aggregated because of restriction of intermolecular rotation (RIR).¹⁵ Previously, we prepared amphiphilic polymeric micelles as a visible drug delivery system with low cytotoxicity and superior imaging quality.¹⁶ The micelles were comprised of amino-methoxypolyethylene, which provided the hydrophilic arms, and tetraphenylethene (TPE), an archetypal AIE luminogen), which provided the hydrophobic imaging moieties. Tang's group also took advantage of the unique "turn on" fluorescence of AIE molecules and fabricated a fluorogenic probe by attaching large amounts of TPE to a chitosan (CS) chain.¹⁷ The resultant TPE-CS bioconjugate exhibited bright emission when the molecules were aggregated, and the aggregates were easily taken up into cells, where they remained detectable for as long as 15 passages. All this evidence indicates that TPE possesses hydrophobicity with high biocompatibility, good photo-stability and accessible functionalization.

Herein, to overcome the poor performance of cationic polymers in gene delivery while adding the advantages of a hydrophobic AIE luminogen, we conjugated polyethyleneimine (PEI) with carboxylated TPE (TPE-COOH) and palmitic acid (PA). PA was introduced here to provide a larger hydrophobic

segment than TPE alone. As shown in Scheme 1, the conjugate (abbreviated as TPEI) was designed to self-assemble into micelle-like nanoparticles (TPEI-NPs) in aqueous media and display bright emission for long-term tracking. In addition, we predicted that nucleic acids would interact with TPEI-NPs through electronic adsorption and would be transferred efficiently into cells with low cytotoxicity.



Scheme 1 Synthetic route of TPEI and schematic illustration of the self-assembly of TPEI nanoparticles (TPEI-NPs).

Results and Discussion

Synthesis and characterization of TPEI

As the gold standard for effective gene transfection, 25 kDa branched PEI was chosen as the skeleton of the cationic polymer. TPEI was synthesized simply by conjugating TPE-COOH and PA to PEI via amide linkage. The molar ratios between primary amino on PEI and carboxyl groups were 10:1, 20:1, and 40:1 (denoted as 10-1 TPEI, 20-1 TPEI, and 40-1 TPEI), with TPE-COOH and PA contributing equal amounts of carboxyl groups. According to the ^1H NMR characterization shown in Figure S1-S4, the appearance of new peaks at 1.26 ppm and 7.30 ppm suggested that the PEI skeleton was successfully modified with hydrophobic segments, and their integrals indicated that the degrees of substitution were 1.25% for 10-1 TPEI, 0.96% for 20-1 TPEI and 0.71% for 40-1 TPEI respectively. Moreover, it could be learned from ^1H NMR spectrums that the molar ratio of TPE-COOH and PA was about 1:3 on per-molar PEI modification, thus molecular weights of 10-1 TPEI, 20-1 TPEI and 40-1 TPEI were calculated as 27130, 26639 and 26216 respectively. The solid TPEI powders had a faint yellow colour under daylight, and became emissive when excited by a UV light (Fig. 1A). The blue fluorescence intensified as the ratio of TPE increased. 10-1 TPEI powder showed the highest intensity of fluorescence, which is 1.41 times that of 20-1 TPEI powder and 1.75 times that of 40-1 TPEI under the same mass (Figure S5). This result confirmed the successful modification of PEI by the TPE moiety with increasing feed ratios. It also suggested that TPEI has characteristics of AIE rather than ACQ, as a powdered polymer labelled with an ACQ fluorescent dye would show a dramatically weakened emission as the degree of labelling increased.¹⁷

The AIE behaviour of TPEI was further investigated spectroscopically. In a benign solvent (DMSO), TPEI (100 $\mu\text{g}/\text{ml}$) dissolved completely and showed rather weak fluorescence due to the free intramolecular rotation of the phenyl rings of TPE. The fluorescence intensity of TPEI rose dramatically as the water fraction of the DMSO solution gradually increased (Fig. 1B-D). This is consistent with the RIR mechanism, and suggests that TPEI shows typical AIE characteristics. It is notable that, unlike other TPE derivatives reported previously, TPEI still showed faint emission in the benign solvent and its fluorescence increased nonlinearly when water was gradually added. The polymer chain might tangle with and enwrap TPE fluorogen, thus strengthening the RIR process.¹⁸

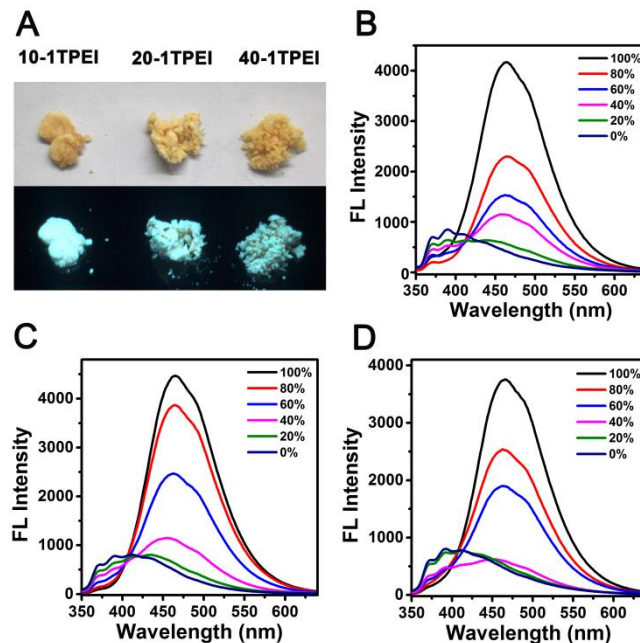


Fig. 1 AIE behaviors of TPEI. (A) Fluorescent images of TPEI under daylight (upper panel) and UV-light (bottom panel). Fluorescence spectra of (B) 10-1 TPEI, (C) 20-1 TPEI and (D) 40-1 TPEI (100 $\mu\text{g}/\text{ml}$) in DMSO/water mixtures with different water fractions (vol %) ($\lambda_{\text{exc}} = 330$ nm).

Preparation and characterization of TPEI-NPs

Based on its amphiphilic properties, TPEI should self-assemble into TPEI-NPs in aqueous media, and this process should induce intense emission due to the RIR of TPE. This sudden increase in fluorescence is convenient for measuring the critical micelle concentration (CMC) of TPEI. As shown in Fig. 2A, 10-1 TPEI, 20-1 TPEI and 40-1 TPEI had different CMCs of 12 $\mu\text{g}/\text{ml}$, 24 $\mu\text{g}/\text{ml}$ and 96 $\mu\text{g}/\text{ml}$ respectively. Fluorescence images of the different polymer solutions (100 $\mu\text{g}/\text{ml}$), shown in the inset of Figure 2A, indicates that 10-1 TPEI and 20-1 TPEI can aggregate in aqueous media and provide efficient fluorescence for cell imaging. A higher concentration of 40-1 TPEI is needed for formation of aggregates. Based on these results, only 10-1 TPEI and 20-1 TPEI were used in the subsequent experiments, because the aggregates are stable at a lower concentration and are less likely to be cytotoxic. Next, the morphologies of 10-1 TPEI-NPs and 20-1 TPEI-NPs were imaged by transmission electron microscopy (TEM) (Fig. 2B and C), and size distributions (Fig. 2D and E) and zeta

potentials were measured via dynamic light scattering (DLS). Above the CMC, both 10-1 TPEI and 20-1 TPEI self-assembled into tight and uniform aggregates with good optical performance. The zeta potentials were 40.1 mV for 10-1 TPEI-NPs and 45.3 mV for 20-1 TPEI-NPs. Thus, the aggregates have a high positive charge, which lay the foundation for electrostatic interactions with negatively charged nuclei acids.

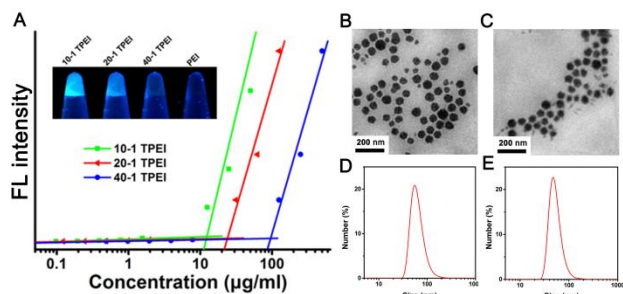


Fig. 2 Characterization of TPEI-NPs. (A) Measurement of the critical micelle formation concentration (CMC). Inset: Fluorescent images of TPEI and PEI solutions (100 $\mu\text{g}/\text{ml}$). TEM images of (B) 10-1 TPEI-NPs and (C) 20-1 TPEI-NPs, and their respective size distributions (D and E).

Characterization of complexes

To investigate the potential of TPEI-NPs in gene delivery and transfection, we chose plasmid DNA (pDNA) encoding green fluorescent protein (GFP) as a model nucleic acid. An important parameter of the carrier in a gene delivery system is the ability to bind pDNA and condense it into complexes. Herein, agarose gel electrophoresis was performed to characterize the complexes of TPEI-NPs and pDNA at different N/P ratios, and the particle sizes and zeta potentials were also determined. For the sake of simple calculation of N/P ratio, the amount of amino groups on TPEI were considered to be same as PEI with the low grafting degree of hydrophobic groups on PEI. As shown in Fig. 3, the results indicated that the introduction of hydrophobic segments affected the ability of TPEI-NPs to bind and condense pDNA. 10-1 TPEI-NPs inhibited pDNA migration at an N/P ratio of 6, while 20-1 TPEI-NPs required an N/P ratio of 4. These results can be compared with a previous report that 25 kD PEI completely retards pDNA migration at an N/P ratio of just 2.¹⁹ The different binding affinity for pDNA might be due to the different level of free amino groups on the polycations. In 10-1 TPEI, more of the PEI amino groups were coupled with TPE and PA. The zeta potentials of complexes showed an upward trend as the N/P ratios increased. The 10-1 TPEI-NPs/pDNA and 20-1 TPEI-NPs/pDNA complexes got the smallest size at an N/P ratio of 10. It is worth noting that the 20-1 TPEI-NPs/pDNA complexes were smaller in size at all the N/P ratios tested, which might result in higher gene transfection efficiency.

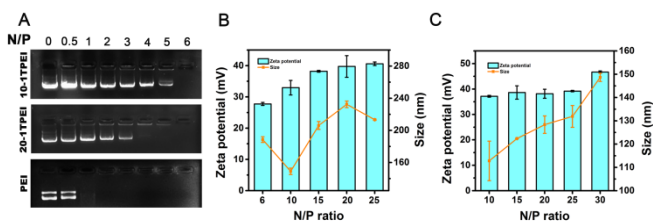


Fig. 3 (A) Agarose gel electrophoresis assay of TPEI-NPs/pDNA complexes. Sizes and zeta potentials of (B) 10-1 TPEI-NPs/pDNA complexes and (C) 20-1 TPEI-NPs/pDNA complexes at different N/P ratios.

Biocompatibility *in vitro*

To demonstrate the biocompatibility of TPEI-NPs *in vitro*, their cytotoxicity to cells from the human embryonic kidney cell line 293T was evaluated by MTT assay. As shown in Fig. 4A, cells treated with 10-1 and 20-1 TPEI-NPs displayed high viabilities at all the tested concentrations. For PEI, the parental cationic polymer, the cell viabilities dropped sharply at high concentrations. When TPEI-NPs and PEI were mixed with a fixed amount of pDNA (0.1 μg) at different N/P ratios, the 10-1 and 20-1 TPEI-NPs/pDNA complexes showed much better biocompatibility (Fig. 4B), while the PEI/pDNA complexes gradually became more toxic with increasing N/P ratios. The toxicity of PEI arises mainly from the strong interaction between the positively charged polymer and the negatively charged cell membrane, which subsequently disrupts the membrane.²⁰ The introduction of hydrophobic segments helps to reduce this undesired toxicity due to the hydrophobic interaction with cell membrane conferred to the resulting amphiphilic polycation derivatives and the enhancement of cell uptake.^{21, 22} Therefore, TPE modified PEI showed much lower cytotoxicity than its parental polymer, a crucial property for subsequent cell-based experiments.

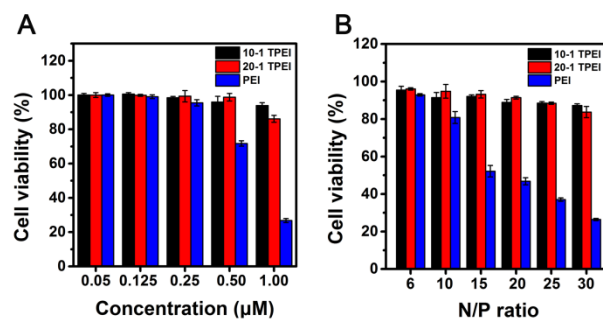


Fig. 4 Evaluation of the toxicity of TPEI and PEI at different concentrations (A) and of the binary complexes at different N/P ratios (B) using 293T cells.

Cell imaging

Next, to test whether TPEI-NPs are suitable for cell imaging, we treated 293T cells with 10-1 or 20-1 TPEI-NPs and observed them by confocal laser scanning microscopy (CLSM). As shown in Fig. 5A, the TPEI-NPs treated cells displayed obvious blue fluorescence in the cytoplasm. Lysosomes were further stained with LysoTracker® Deep Red to identify the subcellular localization of the TPEI-NPs. The fluorescence overlap between TPEI-NPs and LysoTracker® Deep Red indicated that TPEI-NPs were efficiently internalized by cells and mainly accumulated in the perinuclear area. TPEI-NPs were then studied as a vehicle to deliver pDNA encoding GFP. 293T cells were treated with 10-1 and 20-1 TPEI-NPs/pDNA complexes and then imaged by CLSM. 24 h after transfection, when GFP was expressed and showed green fluorescence, the blue fluorescence of TPEI-NPs in the cellular cytoplasm remained visible (Fig. 5B). This suggested that TPEI-NPs can deliver pDNA efficiently and serve as bioprobes for long-term

cell tracking. Thus, TPEI-NPs provide an optical tool for real-time and long-term tracing of gene delivery and transfection.

Transfection *in vitro*

Even though TPEI-NPs show high biocompatibility and good optical properties in cells, they also need to guarantee transfection efficiency similar to PEI, which has the highest transfection efficiency at an N/P ratio of 10,²³⁻²⁵ in order to be useful in future applications. Flow cytometry was used to evaluate the transfection efficiency of TPEI-NPs/pDNA complexes at different N/P ratios from 6 to 30 (Fig. 6A). The results indicated that 20-1 TPEI-NPs/pDNA complexes showed higher transfection efficiency than 10-1 TPEI-NPs/pDNA complexes at all tested N/P ratios. For both 10-1 and 20-1 TPEI-NPs/pDNA complexes, the greatest transfection efficiency was observed when the N/P ratio was 10. The better transfection efficiency of 20-1 TPEI-NPs might result from the higher level of free groups on the backbone, which would offer better pDNA binding capacity and enhance the formation of small, compact polyplexes as indicated by DLS measurements.⁷ Fluorescence microscope was utilized to examine 293T cells transfected with 10-1 and 20-1 TPEI-NPs/pDNA complexes at their optimized N/P ratio of 10. As shown in Fig. 6B-6D, cells treated with 10-1 TPEI-NPs/pDNA complexes expressed a low level of GFP and exhibited weak green fluorescence. However, cells treated with 20-1 TPEI-NPs/pDNA complexes and 25 kDa PEI/pDNA complexes showed bright green emission due to high expression of GFP.

Fig. 5 (A) CLSM images of 293T cells treated with TPEI-NPs. Lysosomes, stained by LysoTracker® Deep Red, exhibited red emission. (Scale bar = 20 μm) (B) CLSM images of 293T cells treated with 10-1 and 20-1 TPEI-NPs/pDNA complexes for 24 h. (scale bar = 10 μm).

Conclusions

In conclusion, we designed and successfully synthesized TPEI (PEI modified with the AIE luminogen TPE) to tackle the problem of undesired cytotoxicity of cationic polymers used for gene transfection, and also to provide an optical tool for cellular imaging of the gene delivery process. Following the incorporation of hydrophobic TPE and PA, TPEI can self-assemble into micelle-like nanoparticles (TPEI-NPs) above the CMC. The TPEI-NPs exhibit bright blue emission based on the RIR of the TPE moieties, and this fluorescence was utilized for real-time and long-term cell imaging. TPEI-NPs have uniform morphologies and a high positive charge, and can bind and condense pDNA efficiently. Compared with PEI, the hydrophobic conjugation dramatically improved the biocompatibility of the cationic polymer, while the transfection efficiency of 20-1 TPEI-NPs remained as high as that of 25 kDa PEI. These features and capabilities of TPEI represent a major step toward designing gene delivery systems with low toxicity and high visibility.

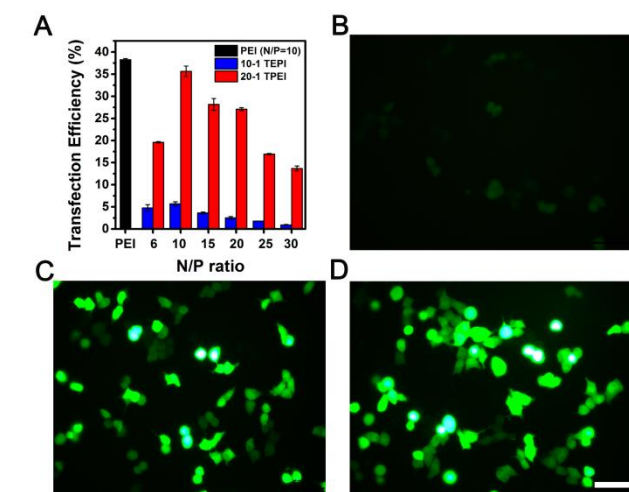
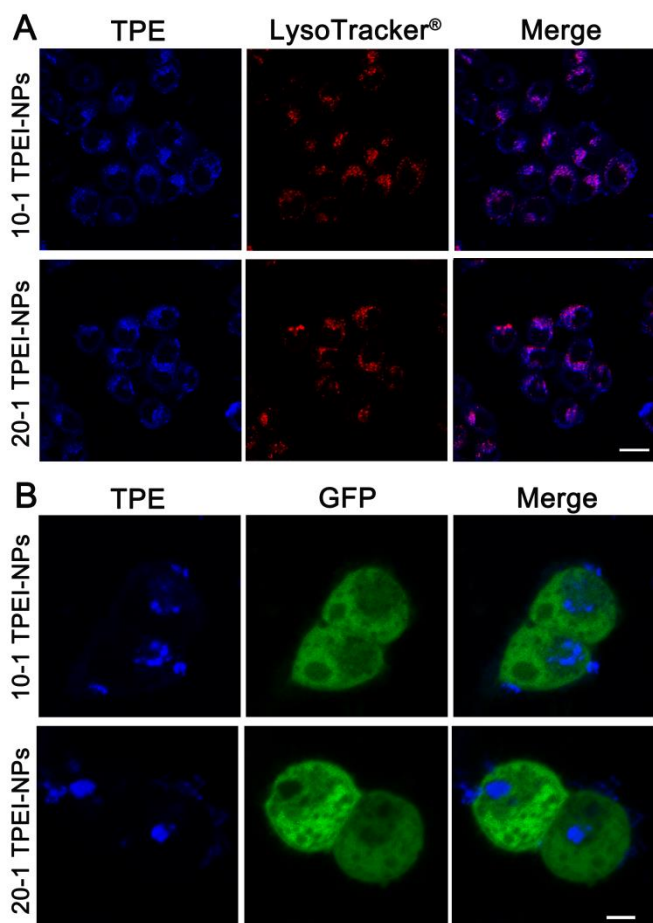


Fig. 6 (A) Evaluation of the expression of GFP in 293T cells using flow cytometry. Fluorescence microscopy of 293T cells transfected by (B) 10-1 TPEI-NPs/pDNA, (C) PEI/pDNA and (D) 20-1 TPEI-NPs/pDNA *in vitro* (N/P=10, scale bar = 50 μm).

Experimental section

Materials

O-(7-azabenzotriazole-1-yl)-1,1,3,3-tetramethyluronium hexafluorophosphate (HATU) and diisopropylethylamine (DIEA) were purchased from BO MAI JIE Technology Co., Ltd (Beijing, China). Branched PEI (MW=25 kDa), dimethyl formamide (DMF), dimethyl sulfoxide (DMSO), ethidium bromide, agarose, and 3-[4, 5-dimethylthiazol-2-yl]-2, 5-diphenyltetrazolium bromide (MTT) were purchased from Sigma Aldrich (St. Louis, MO). LysoTracker® Deep Red was purchased from Molecular Probes Inc. (Eugene, OR, USA). EGFP-N1 plasmid (4700 bp) was supplied by Clontech

Laboratories, Inc. (Mountain View, CA). The human embryonic kidney cell line 293T was obtained from American Type Culture Collection (ATCC, Manassas, VA). Cell culture medium and fetal bovine serum were from Wisent Inc. (Multicell, Wisent Inc., St. Bruno, Quebec, Canada). 0.25% Trypsin-EDTA and antibiotic solutions of penicillin and streptomycin were obtained from Invitrogen (Invitrogen, Carlsbad, CA). Culture dishes and plates were purchased from Corning (Corning, New York, USA).

Synthesis of TPEI

In order to obtain TPEI, carboxylated tetraphenylethylene (TPE-COOH) was first synthesized according to our previously published procedures.²⁶ To synthesize TPEI, equimolar TPE-COOH and PA were dissolved in DMF at room temperature. HATU and DIEA were then added to the solution, which turned yellow after stirring for 3 min. According to the different feed ratios, TPE-COOH and PA solutions were added dropwise into PEI solution in DMF and the mixture stirred continuously at room temperature for 48 h. The product solution was precipitated by cold diethyl ether and the precipitation was then dissolved in 2 mL TFA, subsequently precipitated by cold diethyl ether again to remove the TPE-COOH and PA. Next, to remove the PEI, the precipitation was dissolved in the solution of DMF/H₂O (1:100) and then dialyzed with a molecular weight cutoff of 34 kDa. The pure product was lyophilized and analysed by nuclear magnetic resonance (NMR, AVANCE III, Bruker Biospin).

Determination of the critical micelle formation concentration (CMC) of TPEI-NPs

The CMC of 10-1, 20-1 and 40-1 TPEI was determined by detecting the sudden increase in TPE fluorescence when TPEI assembled into aggregates in aqueous media. A series of TPEI solutions with concentrations from 0.1 µg/mL to 300 µg/mL were placed in vials then sonicated for 10 min. Then fluorescence intensity at a wavelength of 460 nm (excited at 330 nm) was evaluated using a fluorescence spectrophotometer (LS55, Perkin Elmer). A graph was plotted of the fluorescence intensity as a function of TPEI concentration and the CMC was obtained from the junction of the two linear portions.

Preparation and characterization of TPEI-NPs

A solvent displacement method was used to prepare TPEI-NPs. TPEI was dissolved in DMSO and the DMSO solution was added dropwise into distilled water under sonication for 10 min. The mixture was then placed in a dialysis bag (Mn=10 kD) and dialyzed against water to remove DMSO for 24 h. After the TPEI-NPs had formed, their size distributions and zeta potentials were determined using a Zetasizer 5000 (Malvern Instruments, Malvern, Worcestershire, U.K.), and the morphologies were imaged using a Tecnai G2 20 transmission electron microscope (TEM) with 200 kV acceleration voltage.

Preparation and characterization of TPEI-NPs/pDNA complexes

The N/P ratios of complexes were calculated as the molar ratio of the amino groups (N) on TPEI to the phosphate groups (P) on the plasmid DNA (pDNA). pDNA (1 µg/50 µl) was mixed using a pipette with 50 µl of TPEI-NPs at different N/P ratios to form binary complexes. All the complexes were incubated for 30 min at room temperature before being used in experiments. An agarose gel electrophoresis was performed to

evaluate the DNA binding and condensing ability of TPEI-NPs and the stability of the complexes. 10 µl of TPEI-NP/pDNA complex solution was mixed with 2 µl 6 × loading buffer, and 10 µl of the mixture was loaded into a 0.8% (wt) agarose gel containing 0.5 µg/ml ethidium bromide. Electrophoresis was performed in 1 × TAE buffer at 120 V for 20 min. DNA retardation was analysed under UV light at a wavelength 254 nm to visualize the DNA, and the images were obtained using an Image Master VDS Thermal Imaging System (Bio-Rad, CA). Based on the results of agarose gel electrophoresis, the size distributions and the zeta potentials of TPEI-NP/pDNA complexes at different ratios were measured using a Zetasizer Nano ZS (Malvern Instrument, Inc., Worcestershire, UK), and the morphologies of the complexes were investigated via TEM.

Cell culture

The human embryonic kidney cell line 293T was maintained in Dulbecco's modified Eagle's medium/high glucose with 10% fetal bovine serum in a humidified atmosphere containing 5% CO₂ at 37 °C.

Cytotoxicity studies by MTT assay

293T cells were seeded at 5×10^3 cells per well in a 96-well plate, incubated for 24 h, and then cultured for another 24 h with TPEI-NPs at different concentrations ranging from 0.05 µM to 1.00 µM or with TPEI-NP/pDNA complexes at different N/P ratios. The cell culture medium was replaced with 100 µl 0.5 mg/ml MTT and 3 h later the MTT solution was replaced by 100 µl DMSO solution. The results were evaluated by the absorbance measured at 570 nm versus a reference wavelength of 630 nm using an Infinite M200 microplate reader (Tecan, Durham, USA). Untreated cells in medium were used as a control and all experiments were performed with three replicates. The cytotoxicity of PEI and PEI/pDNA complexes were evaluated by the same method.

Confocal laser scanning microscope imaging

293T cells were seeded at 1×10^5 cells per dish in a 35 mm glass dish, pre-incubated for 24 h in complete DMEM and then incubated with TPEI-NPs for 3 h at 37 °C. Cells were then washed three times with PBS and stained with LysoTracker® Deep Red (diluted 1000 times in PBS) for 12 min. Cells were then washed a further three times with PBS and imaged using a confocal laser scanning microscope (PerkinElmer UltraVIEW VoX) with excitation at 405 nm for TPE and 630 nm for LysoTracker® Deep Red. To confirm the capacity of TPEI-NPs to delivery and track gene delivery effectively, cells were washed with PBS and incubated in 1 ml of reduced serum Opti-MEM, to which complexes were added containing 1 µg pEGFP-N1 plasmid at an N/P ratio of 10. After 4 h incubation at 37 °C in a 5% CO₂ humidified atmosphere, the transfection medium was removed and replaced with serum-containing medium for a further 20 h of incubation. Subsequently, cells were washed with PBS, stained with Lyso Tracker® Deep Red for 10 min, and washed with PBS again. After that, cells were imaged under a confocal laser scanning microscope (CLSM) (LSM 710, Carl Zeiss Microscope Co. Ltd., Germany).

In vitro plasmid transfection

The pEGFP-N1 plasmid was utilized to assess the transfection efficiency of binary complexes. PEI/pDNA

(N/P=10) was used as the positive control. 293T cells were seeded at 5×10^4 cells per well in a 24-well plate and incubated for 24 h, and then the complete medium was replaced with Opti-MEM. Subsequently, complexes containing 1 μ g pEGFP-N1 plasmid at different N/P ratios were added to each well. Each transfection was carried out with three replicates. After incubation for 4 h at 37 °C in a 5% CO₂ humidified atmosphere, the transfection solution was removed and replaced by fresh DMEM containing 10% FBS. The cells were incubated for another 24 h under the same conditions. Cells were then obtained by treatment of Trypsin-EDTA, and transfection efficiency was determined using an Attune® acoustic focusing cytometer (Applied Biosystems, Life Technologies, Carlsbad, CA). After that, an inverted fluorescence microscope (Olympus IX 70, Olympus, Tokyo, Japan) was utilized to examine 293T cells that were transfected with 10-1 and 20-1 TPEI-NP/pDNA complexes at their optimized N/P ratio of 10, and micrographs were obtained with Cool SNAP-Pro (4.5.1.1) software.

Acknowledgements

This work was supported by the Chinese Natural Science Foundation project (81171455, 31170873), National Distinguished Young Scholars grant (31225009) from the National Natural Science Foundation of China, National Key Basic Research Program of China (2009CB930200), CAS Knowledge Innovation Program and State High-Tech Development Plan (2012AA020804, 2012AA022502 and SS2014AA020708). The authors also appreciate the support by the external cooperation program of BIC, Chinese Academy of Science, Grant No. 121D11KYSB20130006 and the "Strategic Priority Research Program" of the Chinese Academy of Sciences Grant No. XDA09030301.

Notes and references

^a CAS Key Laboratory for Biological Effects of Nanomaterials & Nanosafety, National Center for Nanoscience and Technology, No. 11 Beiyitiao, Zhongguancun, Beijing 100190, China. Fax: +86-010-62656765; Tel: +86-010-82545530; E-mail: zhangcq@nanoctr.cn, xujing@nanoctr.cn and liangxj@nanoctr.cn.

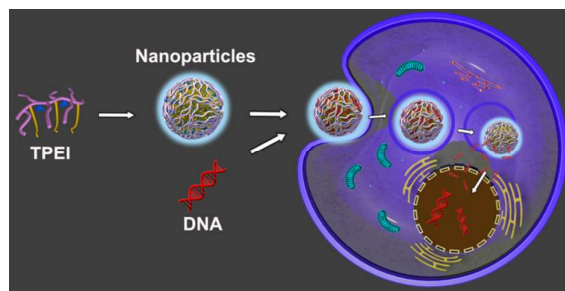
^b State Key Laboratory of Natural Medicines, Department of Pharmaceutics, China Pharmaceutical University, Nanjing 210009, China.

† Keni Yang and Shengliang Li, contributed equally to this work.

Electronic Supplementary Information (ESI) available: ¹H NMR characterization of TPEI (Fig. S1-S4). See DOI: 10.1039/b000000x/

- Ronald G. R., *Science*, 1995, **270**, 404-410.
- Langer, R.; Tirrell, D. A., *Nature*, **2004**, 428, 487-492.
- Samal, S. K.; Dash, M.; Van Vlierbergh, S.; Kaplan, D. L.; Chiellini, E.; Van Blitterswijk, C.; Moroni, L.; Dubruel, P., *Chem. Soc. Rev.*, 2012, **41**, 7147-7194.
- Wang, M.; Liu, H.; Li, L.; Cheng, Y., *Nat. Commun.*, 2014, **5**, 1-8.
- Park, T. G.; Jeong, J. H.; Kim, S. W., *Adv. Drug. Deliver. Rev.*, 2006, **58**, 467-486.
- Liu, Z.; Zhang, Z.; Zhou, C.; Jiao, Y., *Prog. Polym. Sci.*, 2010, **35**, 1144-1162.
- Tian, H.; Xiong, W.; Wei, J.; Wang, Y.; Chen, X.; Jing, X.; Zhu, Q., *Biomaterials*, 2007, **28**, 2899-2907.
- Alshamsan, A.; Haddadi, A.; Incani, V.; Samuel, J.; Lavasanifar, A.; Uludag, H., *Mol. Pharm.*, 2008, **6**, 121-133.
- Liu, G.; Swierczewska, M.; Lee, S.; Chen, X., *Nano Today*, 2010, **5**, 524-539.
- Feng, X.; Lv, F.; Liu, L.; Yang, Q.; Wang, S.; Bazan, G. C., *Adv. Mater.*, 2012, **24**, 5428-5432.
- Hong, Y.; Lam, J. W.; Tang, B. Z., *Soc. Rev.*, 2011, **40**, 5361-5388.
- Svenson, S.; Tomalia, D. A., *Adv. Drug. Deliver. Rev.* 2012, **64**, 102-115.
- Dubertret, B.; Skourides, P.; Norris, D. J.; Noireaux, V.; Brivanlou, A. H.; Libchaber, A., *Science*, 2002, **298**, 1759-1762.
- Smith, A. M.; Duan, H.; Mohs, A. M.; Nie, S., *Adv. Drug. Deliver. Rev.*, 2008, **60**, 1226-1240.
- Hong, Y.; Lam, J. W.; Tang, B. Z., *Chel. Commun.*, 2009, **29**, 4332-4353.
- Zhang, C.; Jin, S.; Li, S.; Xue, X.; Liu, J.; Huang, Y.; Jiang, Y.; Chen, W.-Q.; Zou, G.; Liang, X.-J., *ACS Appl. Mater. Inter.*, 2014, **6**, 5212-5220.
- Wang, Z.; Chen, S.; Lam, J. W.; Qin, W.; Kwok, R. T.; Xie, N.; Hu, Q.; Tang, B. Z., *J. Am. Chem. Soc.*, 2013, **135**, 8238-8245.
- Hu, R.; Leung, N. L.; Tang, B. Z., *Chem. Soc. Rev.*, 2014, **43**, 4494-4562.
- Erbacher, P.; Bettinger, T.; Belguisse - Valladier, P.; Zou, S.; Coll, J. L.; Behr, J. P.; Remy, J. S., *J. Gene. Med.*, 1999, **1**, 210-222.
- Godbey, W.; Wu, K. K.; Mikos, A. G., *J. Control. Release.*, 1999, **60**, 149-160.
- Wong, S. Y.; Pelet, J. M.; Putnam, D., *Prog. Polym. Sci.*, 2007, **32**, 799-837.
- Thomas, M.; Klibanov, A. M., *P. Natl. Acad. Sci. USA.*, 2002, **99**, 14640-14645.
- Guo, S.; Huang Y.; Wei T.; Zhang W.; Wang W.; Lin D.; Zhang X.; Kumar A.; Du Y.; Xing J.; Deng L.; Liang Z.; Wang P. C.; Dong A.; Liang X.-J., *Biomaterials*, 2011, **32**, 879-889.
- Kawabata, A.; Baoum, A.; Ohta, N.; Jacquez, S.; Seo, G. M.; Berkland, C.; Tamura, M., *Cancer. Res.*, 2012, **72**, 2057-2067.
- Khan, M.; Ang, C. Y.; Wiradharma, N.; Yong, L. K.; Liu, S.; Liu, L.; Gao, S.; Yang, Y.-Y., *Biomaterials*, 2012, **33**, 4673-4680.
- Zhang, C.; Liu, C.; Xue, X.; Zhang, X.; Huo, S.; Jiang, Y.; Chen, W.-Q.; Zou, G.; Liang, X.-J., *ACS Appl. Mater. Inter.*, 2013, **6**, 757-762.

Table of Contents



Luminescent nanoparticles (TPEI) were synthesized to tackle the undesired cytotoxicity of cationic polymers and also were used for visible gene transfection.